Energy & Environmental Science

PAPER

View Article Online
View Journal | View Issue

Operando electron magnetic measurements of Li-ion batteries†

Cite this: *Energy Environ. Sci.*, 2014, 7, 2012

Received 12th February 2014
Accepted 19th March 2014

DOI: 10.1039/c4ee00490f

www.rsc.org/ees

Gregory Gershinsky,[a] Elad Bar,[b] Laure Monconduit[c] and David Zitoun*[a]

One of the challenges in the development of batteries consists of investigating new electrode materials and comprehending the mechanism of lithium uptake. Herein, we report on the first *operando* measurements of electron magnetism in a battery during cycling. We have succeeded in designing a non-magnetic cell and have investigated the lithiation mechanism of $FeSb_2$, a high energy density anode material. The stepwise increase of the magnetic moment reveals an increase of amorphous Fe nanoparticle size, while Sb undergoes reversible alloying with Li.

Broader context

Among all rechargeable electrochemical energy storage devices available today, lithium-ion batteries (LIBs) display the highest energy density. Nevertheless, a breakthrough is needed to extend their applications in a wide range of portable devices and transportation vehicles. As an alternative to the commercially available graphite, conversion anode materials display promising characteristics such as high gravimetric and volumetric energy densities. Conversion reactions, where an electrode material undergoes a phase change, present several unique characteristics which make them an interesting scientific topic and also technologically challenging. Each interface is highly reactive; the metastable phases formed during cycling of the battery relax to more stable states, thus questioning the use of *ex situ* measurements on electrodes. *In situ* local probe measurements have been recently developed to understand the lithiation mechanism. In this paper, we report on the first *in situ* measurements of electron magnetism in a battery during cycling. $FeSb_2$, a very interesting anode material for LIBs, displays a high energy density and allows the investigation of its structural evolution during cycling through magnetic measurement.

The rechargeable Li-ion batteries (LIBs) display high energy density which makes them the preferred energy storage devices for portable applications.[1] The performance of LIBs depends on materials evolution upon cycling.[2] One of the challenges consists of investigating new electrode materials and comprehending the mechanism of lithium uptake.[3] New ways to get real-time information on the performances of the battery are continuously sought. The development of *in situ* (or *operando*) characterization techniques provides valuable information on chemical processes while the interpretation of *ex situ* measurements provides a partial picture of the chemical reactions.[4] The electrode lithiation can be described as an intercalation, insertion, conversion or alloying reaction with lithium. The development of effective conversion and alloying electrode materials is a milestone for the achievement of high energy density LIBs required for electrical vehicles (EVs). As an alternative to graphite, conversion anode materials display promising characteristics such as high gravimetric and volumetric capabilities.[5]

Conversion reactions, where an electrode material undergoes a phase change, are highly sensitive to kinetics. Each interface is highly reactive, thus application of an external potential results in metastable amorphous states far from the thermodynamic equilibrium. These transient states must relax to some new thermodynamic state, thus questioning the use of *ex situ* measurements on electrodes. *In situ* local probe measurements have been recently developed to address the lithiation mechanism, including solid-state nuclear magnetic resonance (SS-NMR),[6] Raman spectroscopy,[7] mass spectrometry,[8] Mössbauer spectrometry,[9] X-ray diffraction,[10] soft X-ray spectroscopy,[11] or electron microscopy.[12] In particular, SS-NMR has been used for the characterization of electrode materials[13] and for the probe of the chemical environment in electrodes *in situ*,[14] while MRI has allowed mapping batteries *operando*,[15] and SS-NMR has been recently applied to paramagnetic solids.[16] Indeed, most of the electrode materials are based on Mn, Fe, Co or Ni. Even silicon, a promising anode material can be alloyed with a transition metal to improve its cycling ability. The electrodes display a paramagnetic or ferromagnetic behavior at one stage during the lithiation or delithiation process which makes electron magnetic measurements highly valuable as shown by the *ex situ* measurements on pristine and cycled electrode

[a]*Department of Chemistry, Bar Ilan Institute of Nanotechnology and Advanced Materials (BINA), Ramat Gan 52900, Israel. E-mail: david.zitoun@biu.ac.il*

[b]*Department of Physics, Bar Ilan Institute of Nanotechnology and Advanced Materials (BINA), Ramat Gan 52900, Israel*

[c]*Institut Charles Gerhardt UMR CNRS 5253, ALISTORE European Research Institute (3104 CNRS) – AIME, Université Montpellier 2, CC1502, place E. Bataillon, 34095 Montpellier cedex 5, France*

† Electronic supplementary information (ESI) available: Control experiments of *operando* magnetic measurements and prolonged cycling. See DOI: 10.1039/c4ee00490f

materials.[17,18] The presence of transition metals in electrodes opens up an avenue for the study of electron magnetic properties to resolve the lithiation mechanism. We have previously reported on the *ex situ* measurements of magnetism in conversion materials for anodes.[19,20] Nevertheless, to the best of our knowledge, no publication has reported *operando* measurements of electron magnetism in LIBs until now.

Operando electron magnetic measurements should provide quantitative information on the electrochemical processes, in particular when a ferromagnetic phase is formed electrochemically, even on amorphous phases. In this framework, we have isolated the model compound $FeSb_2$ by alloying an active anode material Sb with a magnetic transition metal Fe, thus undergoing a conversion process into amorphous Fe and nanocrystalline Li_3Sb.[21]

In this paper, we report on the first *in situ* measurements of electron magnetism in a battery during cycling. We have succeeded in designing a non-magnetic cell and have investigated the lithiation mechanism of $FeSb_2$, which is used as an electrode material. The magnetization has been measured at constant magnetic field or at a sweeping magnetic field in a SQUID magnetometer for several charge–discharge cycles. These real-time measurements change our perception of the lithiation mechanism in $FeSb_2$. After the first cycle, the electrochemical process involves the reversible lithiation of Sb only, while all the changes in the magnetic moment are mainly due to nanostructural effects with an evolution of Fe particle size, leading to a distinct lithiation mechanism.

$FeSb_2$ is a very interesting anode material for LIBs, due to both its performance and the ability to study Fe and Sb by Mössbauer spectrometry.[22] The low polarization value and the highly stable potential of $FeSb_2$ stand close to the performance of insertion materials at 0.8 V, with better volumetric and gravimetric values than graphite (4100 mA h cm^{-3}; 540 mA h g^{-1} for $FeSb_2$ and 820 mA h cm^{-3}; 372 mA h g^{-1} for graphite) and with a coulombic efficiency above 97% (Fig. S3,† charge–discharge capacity). A previous study has shown that the electrochemical reaction is thought to be a reversible conversion process according to the following chemical equations:[22]

$$FeSb_2 + 4Li \leftrightarrow Li_4FeSb_2$$

$$Li_4FeSb_2 + 2Li \leftrightarrow 2Li_3Sb + Fe$$

Fe is the only ferromagnetic phase as the ^{57}Fe Mössbauer spectrum of the ternary phase does not show any magnetic ordering; the temporal evolution of the magnetic moment should give us a quantitative proof of the validity of the proposed mechanism. On the other hand, recent work on conversion electrode materials has demonstrated the instability of the composite electrode formed at the end of lithiation and the necessity of *in situ* measurements.[23]

The *in situ* cell has been designed using diamagnetic raw materials according to the geometrical constraints of a SQUID cryostat with an external diameter of 6.5 mm and a length of 20 mm (Fig. 1B), and inserted in a polypropylene straw (Fig. 1A). The working electrode consists of $FeSb_2$ formulated on a Cu foil and the counter electrode of Li plated on the Cu foil; all details are available in the ESI.† The cell is connected in galvanostatic mode at C/5 from 0 V to 1.4 V and cycled at 300 K while the magnetic moment is sampled at constant field (2 T). In a control experiment, the magnetic measurements were performed on a polypropylene cell assembled without $FeSb_2$. The reference sample displays a constant paramagnetic value (Fig. S1†).

The temporal changes in the magnetic moment of $FeSb_2$ follow the periodicity of the potential (Fig. 1C). The lithiation process induces a sharp increase of magnetic moment with a maximum found slightly after the start of the delithiation process. The magnetic moment remains almost constant until a new lithiation process induces another sharp increase. The stepwise increase of the magnetic moment shows damping after 3 cycles. This remarkable behavior is unexpected and resembles the signature of an irreversible phenomenon while the electrochemical processes remain almost steady (Fig. 2A).

In a control experiment, the anode material is tested under the same conditions (rate C/5, the same electrolyte and separator) in standard coin cell configuration *versus* lithium metal. The anode exhibits a reversible capacity of 530 mA h g^{-1} close to the theoretical limit (540 mA h g^{-1}) with two discharge plateaus (0.86 V; 0.78 V) and one charge plateau at 1.02 V. For the sake of consistency, we have plotted the voltage profile collected during the second cycle in the real-time experiment in the same graph

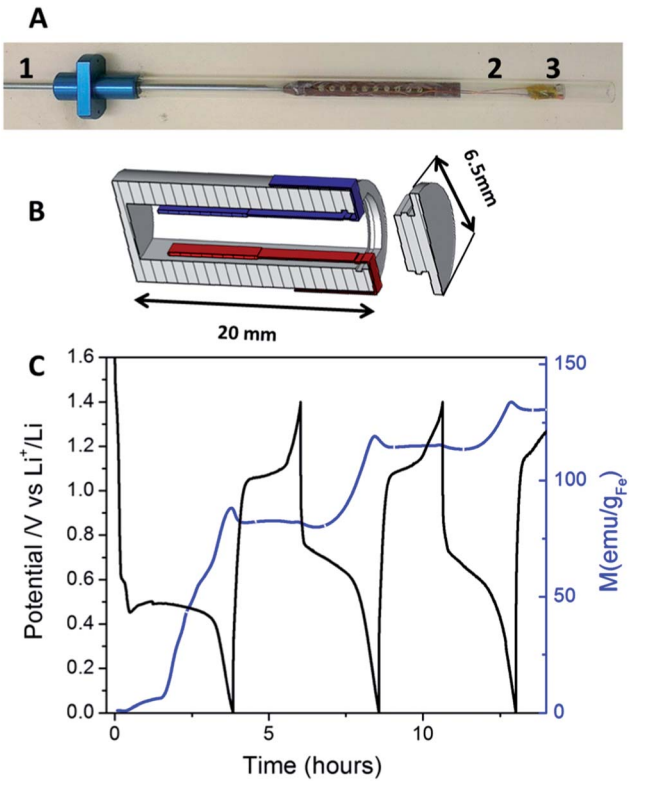

Fig. 1 Photograph of the inset for SQUID measurement (1), the electrical connections (2) and *in situ* cell (3) (A); schematic of the *in situ* cell (B); electrode potential *vs.* lithium during galvanostatic cycling (black) and corresponding magnetic moment at 300 K (blue) (C).

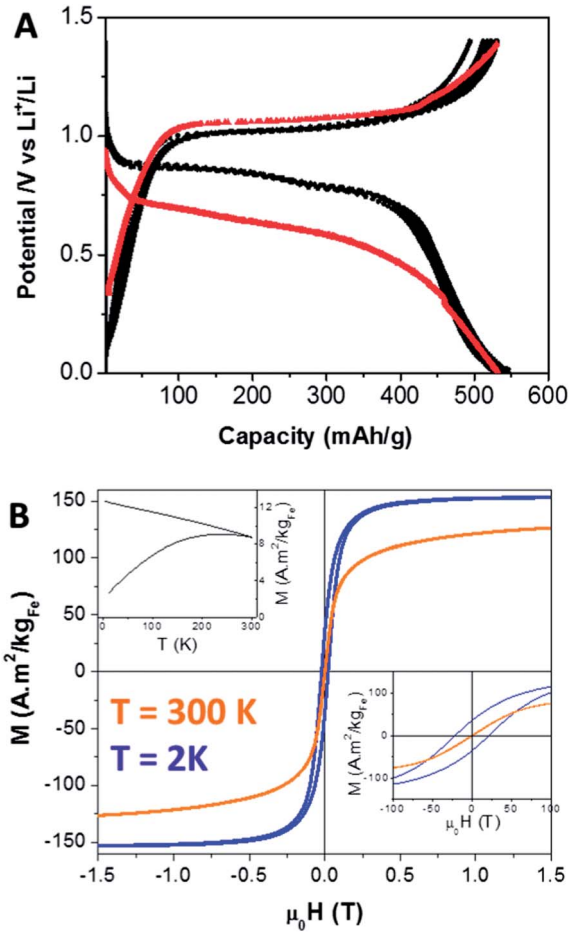

Fig. 2 Electrode potential *vs.* lithium during galvanostatic cycling for the *in situ* cell (red dots) and *ex situ* coin cell (black dots) (A); *ex situ* magnetic measurements after the 8th delithiation: hysteresis at 2 K (blue) and 300 K (orange), magnification of the hysteresis (right down panel) and ZFC/FC (left upper panel) (B).

(Fig. 2A, red line). The *in situ* cell reaches the same capacity with a voltage profile similar to that obtained in the coin cell control experiment (black line). The main discrepancy lies in the higher polarization (potential differences between charge and discharge plateaus), a classical signature for loose pressure between the electrodes in the *in situ* cell. Therefore, electrochemical processes are highly consistent with *ex situ* and *in situ* experiments.

The stepwise increase of the magnetic moment is intriguing and deserves a close investigation of the magnetization as a function of field and temperature. The *ex situ* measurement is performed directly on the $FeSb_2$ electrode of the coin cell after washing and drying in a glovebox. The coin cell is stopped at the end of the delithiation process after 8 cycles; the delithiated electrode should consist of paramagnetic $FeSb_2$ if the conversion mechanism is fully reversible. Nevertheless, the electrode displays a ferromagnetic behavior at 2 K with a high magnetic moment (170 A m^2/kg_{Fe}) (Fig. 2B) and a superparamagnetic behavior at 300 K while the temperature dependence (Zero Field-Cooled/Field-Cooled or ZFC/FC) is typical of superparamagnetic nanoparticles with a maximum in the ZFC around 250 K (Fig. 2B inset). Therefore, the material consists of one phase of nanoscale Fe and one phase consisting mostly of Sb, as already qualitatively demonstrated by Mössbauer spectrometry (Fig. S5†).[22] Both phases are amorphous in the delithiated state and *in situ* XRD experiments have previously shown the occurrence of a Li_3Sb phase only in the discharged electrode, as shown in the ESI (Fig. S4†).

To confirm the superparamagnetic behaviour, we have measured the magnetic moment at constant field during 8 cycles (Fig. 3A) and observed a stepwise increase of the magnetization which reaches a plateau after 8 cycles. Compared to the electrochemical cycle which lasts for 10 hours, a magnetic measurement is very fast (about one second) which allows us to scan the field at a defined potential (around 10 minutes experiment). In Fig. 3A, the stars represent the potential where the magnetization is measured as a function of the field at 300 K. In Fig. 3B, the curves display the expected superparamagnetic behaviour without hysteresis and the magnetic moment does not saturate even at a high field, clearly evidencing the superparamagnetic behaviour. These measurements are consistent with the *ex situ* measurements and demonstrate that low temperature measurements are not needed to confirm the magnetic nature of the materials.

The investigation of a battery is always complex since the electrodes are often very reactive and unstable. The main issue

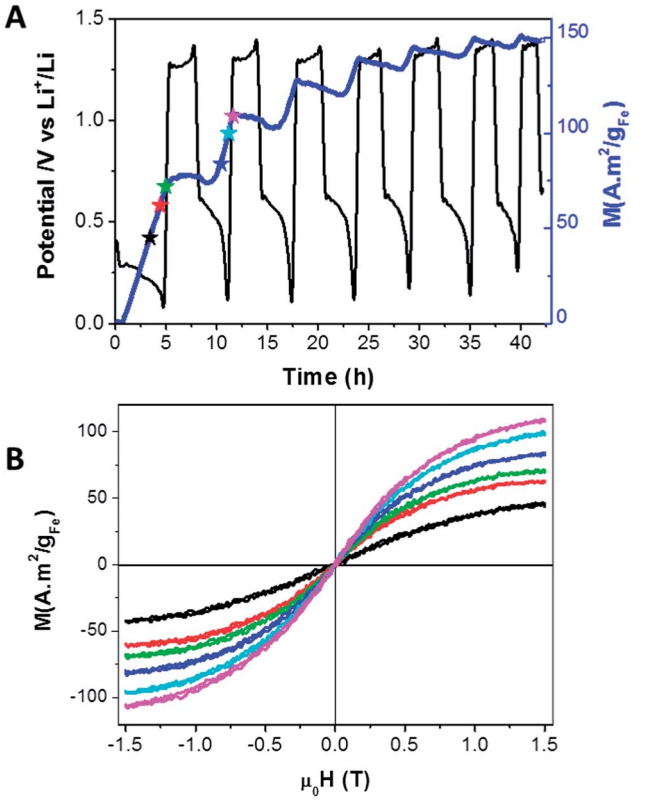

Fig. 3 Electrode potential *vs.* lithium during galvanostatic cycling of the *in situ* cell (plain line) and magnetic moment collected *in situ* at 300 K (blue dots) (A); *in situ* field dependent magnetic measurements; the different colors correspond to the stars on panel A (B).

remains to ensure that the evolution of magnetic properties relates to an electrochemical process and not to a relaxation of the electrode material at constant potential or in open circuit voltage (OCV). Recent work on conversion electrode materials has demonstrated the instability of the composite electrode formed at the end of lithiation.[20] Once the external constraint of an electrochemical potential is lifted, chemical relaxation towards more thermodynamically stable phases or microstructures may occur before one could investigate the electrode using *ex situ* techniques. The *in situ* cell shows no evolution of the magnetic moment with a cell in open circuit voltage (OCV) (Fig. 4A) and at constant potential (CA) without electrochemical processes. The magnetic moment is constant whether the CA or OCV is applied at the end of the lithiation or delithiation process. The magnetic moment follows only the electrochemical processes and does not vary at CA or OCV.

To understand the stepwise increase of the magnetic moment, we have performed several low temperature hysteresis measurements. Each curve displays the magnetic properties of the $FeSb_2$ electrode dried from a battery stopped at a specific state of charge–discharge (Fig. S2A†). During the first lithiation process, the magnetic moment obtained at low temperature increases rapidly to reach the value of 175 A m^2/kg_{Fe}. This magnetic moment is close to the one observed at room temperature after 8 cycles: 150 A m^2/kg_{Fe} (Fig. 3A). From this high magnetic moment, we conclude that the conversion of $FeSb_2$ is already completed after the first lithiation. During *in situ* measurement at 300 K, the magnetic moment reaches only 70 A m^2/kg_{Fe} as a consequence of superparamagnetism.

To verify this point, we have carried out ZFC/FC measurements on the fully delithiated material at the end of charge after *n* cycles (Fig. S2B†). The ZFC/FC curves are characteristic of superparamagnetic behavior with a maximum increasing from $T = 10$ K to $T > 300$ K at the end of the lithiation process. A numerical analysis of the curves according to the Stoner–Wohlfarth model[24] of non-interacting superparamagnetic nanoparticles allows us to calculate the actual radius, while modeling the electrode as Fe magnetic nanoparticles diluted in a non-magnetic matrix.[25] Particle size obtained from ZFC/FC increases linearly upon cycling to more than 8 nm after 10 cycles (Fig. 4B). Fe nanoparticles of this size are above the critical radius and their blocking temperature close to 300 K; the electrode material displays a ferromagnetic behavior.

Operando measurements reveal the complexity of the electrode, which relates to the interplay between the electrochemical reaction and the structural evolution. Contrary to the first proposed schema, the electrochemical reaction is a reversible alloying process based almost exclusively on Sb after first lithiation, following the electrochemical mechanism:

$$2Li_3Sb + Fe \leftrightarrow 2Sb + Fe + 6Li$$

The electrochemical cycle is only based on Sb while Fe phase content remains constant. This mechanism is consistent with the plateau of magnetic moment observed after 8 cycles. Even though Fe does not directly participate in the electrochemical process, the presence of Fe nanoparticles improves the cycling performances of Fe/Sb compared to a Sb electrode with a coulombic efficiency above 97% after the first cycle (500 mA h g^{-1} capacity after 50 cycles in Fig. S3†).

The main magnetic signature of the electrodes results from the nanostructural change in the Fe and Li_xSb phases. The formation of nanoscale Fe is observed already in the first lithiation process and can be considered as an almost complete reaction as demonstrated by the magnetic moment measured at 2 K (Fig. S2A†). Since the particles are very small ($R_{mean} = 3$ nm), the room temperature magnetic moment does not reach the saturation in the *in situ* measurements. Magnetic particle size does not vary at constant potential (at least for 30 minutes), thus allowing for field dependent magnetic measurements. Upon cycling, a steady growth of Fe nanoparticles is observed *in situ* by the stepwise increase of the magnetic moment. This phenomenon results mainly from the magnetic particle size increase and can be explained by the volume expansion during the alloying process of Sb with Li (Fig. 4C).[26] The magnetic moment "waves" are dampened upon cycling when the average magnetic particle size reaches the critical value for superparamagnetic behavior. Further analysis of the detailed relationship between each variation of the magnetic moment and an electrochemical reaction will be carried out by the elaboration of a nanocomposite Fe/Sb material with a specific ratio and particle size.

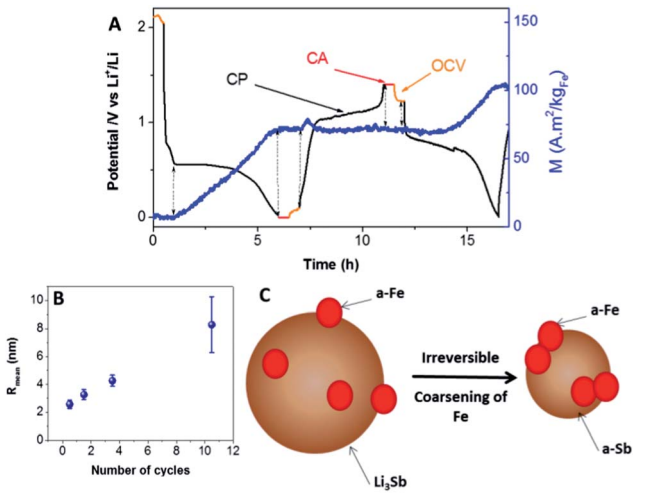

Fig. 4 Electrode potential *vs.* lithium during galvanostatic cycling for the *in situ* cell (black line), open circuit voltage (orange line), constant potential (red line) and magnetic moment at 300 K (blue dots) (A); magnetic particle size calculated from the *ex situ* ZFC/FC measurements as a function of the number of cycles for fully lithiated electrodes (B); schematic of the magnetic size coarsening (C).

Conclusions

The *operando* electron magnetic measurements of LIBs allow us to revisit the electrochemical mechanism of the high energy density anode material $FeSb_2$. The plateau reached by the magnetic moment during *in situ* monitoring implies the

reversible lithiation of Sb only, while the stepwise increase of the magnetic moment at room temperature is caused by the increase of Fe particle size on the first order. *Operando* electron magnetism provides macroscopic and quantitative data on the amorphous Fe nanostructures formed during cycling. The investigation of real-time characterization techniques enables the collection of information at the nanoscale, required to elucidate the electrochemical mechanism. Since most of the electrode materials are based on 3d transition metals with high electron magnetic moment, we believe *in situ* electron magnetic measurements will bring valuable information on the conversion or alloying mechanism to forecast more efficient electrodes.

Acknowledgements

The authors thank Prof. Yossi Yeshurun for his assistance with magnetic measurements and Dr Ali Darwiche for electrochemical measurements. This work was supported by the High Council for Scientific and Technological Cooperation between France and Israel (3-8675) and the I-CORE program of the planning and budgeting committee and the Israel Science Foundation (2797/11).

Notes and references

1 M. Armand and J.-M. Tarascon, *Nature*, 2008, **451**, 652–657.
2 V. Etacheri, R. Marom, R. Elazari, G. Salitra and D. Aurbach, *Energy Environ. Sci.*, 2011, **4**, 3243.
3 J. B. Goodenough, *Acc. Chem. Res.*, 2013, **46**, 1053–1061.
4 S. F. Amalraj and D. Aurbach, *J. Solid State Electrochem.*, 2011, **15**, 877–890.
5 (*a*) M. V. Reddy, G. V. Subba Rao and B. V. R. Chowdari, *Chem. Rev.*, 2013, **113**, 5364–5457; (*b*) L. Ji, Z. Lin, M. Alcoutlabia and X. Zhang, *Energy Environ. Sci.*, 2011, **4**, 2682–2699; (*c*) J. Chen, *Materials*, 2013, **6**, 156–183.
6 M. Letellier, F. Chevallier, C. Clinard, E. Frackowiak, J.-N. Rouzaud, F. Béguin, M. Morcrette and J.-M. Tarascon, *J. Chem. Phys.*, 2003, **118**, 6038–6045.
7 K. Dokko, M. Mohamedi, N. Anzue, T. Itoh and I. Uchida, *J. Mater. Chem.*, 2002, **12**, 3688–3693.
8 L. Gireaud, S. Grugeon, S. Pilard, P. Guenot, J.-M. Tarascon and S. Laruelle, *Anal. Chem.*, 2006, **78**, 3688–3698.
9 R. Fong, C. H. W. Jones and J. R. Dahn, *J. Power Sources*, 1989, **26**, 333–339.
10 A. S. Andersson, B. Kalska, L. Haggstrom and J. O. Thomas, *Solid State Ionics*, 2000, **130**, 41–52.
11 X. Liu, D. Wang, G. Liu, V. Srinivasan, Z. Liu, Z. Hussain and W. Yang, *Nat. Commun.*, 2013, **4**, 2568.
12 J. Y. Huang, L. Zhong, C. M. Wang, J. P. Sullivan, W. Xu, L. Q. Zhang, S. X. Mao, N. S. Hudak, X. H. Liu, A. Subramanian, H. Fan, L. Qi, A. Kushima and J. Li, *Science*, 2010, **330**, 1515–1520.
13 C. P. Grey and N. Dupré, *Chem. Rev.*, 2004, **104**, 4493–4512.
14 E. Blanc, M. Leskes and C. P. Grey, *Acc. Chem. Res.*, 2013, **46**, 1952–1963.
15 S. Chandrashekar, N. M. Trease, H. J. Chang, L. Du and C. P. Grey, *Nat. Mater.*, 2012, **11**, 311–316.
16 D. S. Middlemiss, A. J. Ilott, F. C. Strobridge and C. P. Grey, *Chem. Mater.*, 2013, **25**, 1723–1734.
17 C. M. Julien, A. Ait-Salah, A. Mauger and F. Gendron, *Ionics*, 2006, **12**, 21–32.
18 N. A. Chernova, G. M. Nolis, F. O. Omenya, H. Zhou, Z. Li and M. S. Whittingham, *J. Mater. Chem.*, 2011, **21**, 9865–9875.
19 S. Boyanov, M. Womes, L. Monconduit and D. Zitoun, *Chem. Mater.*, 2009, **21**, 3684–3692.
20 S. Boyanov, D. Zitoun, M. Ménétrier, J. C. Jumas, M. Womes and L. Monconduit, *J. Phys. Chem.C*, 2009, **113**, 21441–21452.
21 J. Xie, X. B. Zhao, G. S. Cao, M. J. Zhao, Y. D. Zhong and L. Z. Deng, *Mater. Lett.*, 2003, **57**, 4673–4677.
22 C. Villevieille, B. Fraisse, M. Womes, J.-C. Jumas and L. Monconduit, *J. Power Sources*, 2009, **189**, 324–330.
23 C. Villevieille, C. M. Ionica-Bousquet, B. Fraisse, D. Zitoun, M. Womes, J. C. Jumas and L. Monconduit, *Solid State Ionics*, 2011, **192**, 351–355.
24 E. Stoner and E. Wohlfarth, *Philos. Trans. R. Soc., A*, 1948, **240**, 599–642.
25 M. Respaud, J. Broto, H. Rakoto, A. Fert, L. Thomas, B. Barbara, M. Verelst, E. Snoeck, P. Lecante, A. Mosset, J. Osuna, T. Ely, C. Amiens and B. Chaudret, *Phys. Rev. B: Condens. Matter Mater. Phys.*, 1998, **57**, 2925–2935.
26 A. Darwiche, C. Marino, M. T. Sougrati, B. Fraisse, L. Stievano and L. Monconduit, *J. Am. Chem. Soc.*, 2012, **134**, 20805–20811.

